

## Electronic Supplementary Information

### **Facile interfacial synthesis of large sized 3D gold spherical architectures with strong single particle SERS response and high reproducibility**

Kaisheng Yao,<sup>a,b</sup> Xinying Li,<sup>a</sup> Yuling Zhao,<sup>a</sup> Weiwei Lu,<sup>b</sup> Jianji Wang<sup>\*a</sup> and Jiongliang Yuan<sup>c</sup>

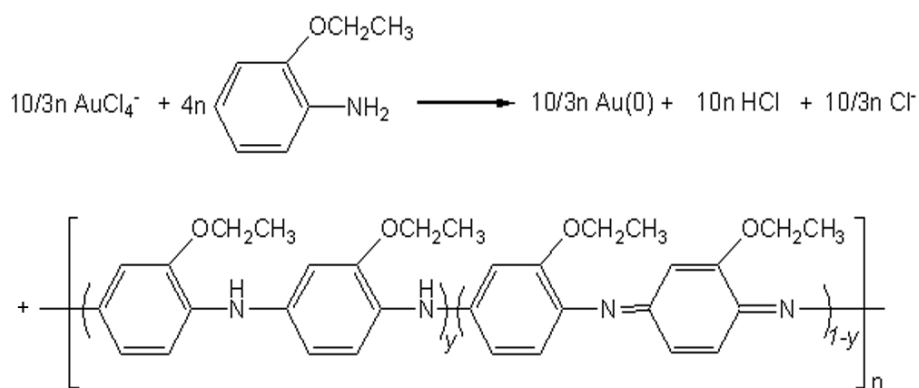
<sup>a</sup>*Collaborative Innovation Center of Henan Province for Green Manufacturing of Fine Chemicals, Key Laboratory of Green Chemical Media and Reactions, Ministry of Education, School of Chemistry and Chemical Engineering, Henan Normal University, Xinxiang, Henan 453007, P. R. China*

<sup>b</sup>*School of Chemical Engineering and Pharmaceutics, Henan University of Science and Technology, Luoyang, Henan 471023, P. R. China*

<sup>c</sup>*Department of Environmental Science and Engineering, Beijing University of Chemical Technology, Beijing 100029, P. R. China.*

\*Author to whom all correspondence should be addressed.

E-mail: [jwang@htu.cn](mailto:jwang@htu.cn)



**Scheme S1** Reaction conversion for the preparation of Au products at the toluene-H<sub>2</sub>O interface.

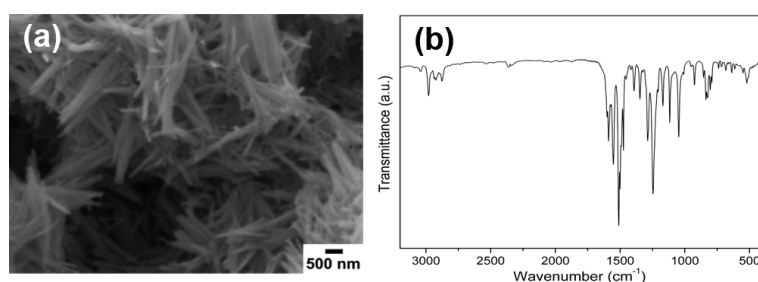


**Fig. S1** (a) SEM image and (b) FT-IR spectra of POEA belts generated during the formation of AuSAs.

Fig. S1a exhibits SEM image of the POEA belt-like structures generated at the toluene-H<sub>2</sub>O interfaces in the course of AuCl<sub>4</sub><sup>-</sup> reduction. Fig. S1b shows the FT-IR spectra of POEA belts polymerized during the formation of Au micro/nanostructures. The absorption related to the C=N on the quinoid ring and the C=C stretching on the benzenoid ring appears at 1552 cm<sup>-1</sup> and 1510 cm<sup>-1</sup>, respectively. The bands at 1286 cm<sup>-1</sup> and 1247 cm<sup>-1</sup> can be attributed to C-N and C-O stretching absorption, respectively. The band at 1169 cm<sup>-1</sup> is assigned to the N=Q=N vibration (Q = quinonoid), and the band at 1117 cm<sup>-1</sup> attributes from C-H in-plane bending vibrations. In addition, the bands at 1392 cm<sup>-1</sup>, 2873 cm<sup>-1</sup> and 2935 cm<sup>-1</sup> are due to -CH<sub>3</sub>-substituted group, while the bands at 2981 cm<sup>-1</sup> and 3045 cm<sup>-1</sup> originate from the C-H stretch on the benzenoid ring. The bands from 1000 to 400 cm<sup>-1</sup> belong to the o-substituted aromatic ring<sup>[1-3]</sup>.

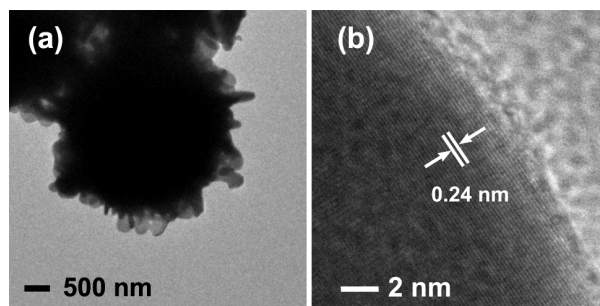


**Fig. S2** TEM (a) and HRTEM (b) images of the AuSAs.

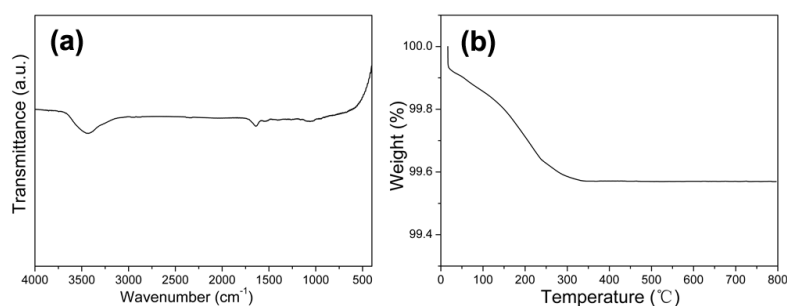


**Fig. S3** (a) FT-IR spectra and (b) TGA curve of the purified AuSAs.

In order to examine if the POEA was completely removed, FT-IR and TGA of the purified AuSAs were performed and the results were shown in Fig. S3. As seen from Fig. S3(a), the main absorption bands at about  $3400\text{ cm}^{-1}$  and  $1600\text{ cm}^{-1}$  could be assigned to O-H stretching and bending vibrations, respectively, indicating that a small amount of water was absorbed on the surface of the purified samples. Nevertheless, Some characteristic peaks of POEA, such as those at  $1286\text{ cm}^{-1}$ ,  $1247\text{ cm}^{-1}$  and  $1169\text{ cm}^{-1}$  which correspond to C-N, C-O and N=Q=N vibrations (Q=quinoniod), respectively,<sup>1-3</sup> did not appear. This suggests that POEA in the samples was completely removed. Next, about 0.4% loss of weight was found from TGA curve of the purified AuSAs shown in Fig. S3(b). The loss of weight mainly occurs with the temperature below about  $300\text{ }^{\circ}\text{C}$ , which can be attributed to the evaporation of water absorbed on the samples. This result is commendably consistent with that of FT-IR spectrum. It can be seen from Fig. 2b in the manuscript that the thermal decomposition of POEA mainly occurs in the temperature range from  $320\text{ }^{\circ}\text{C}$  to  $600\text{ }^{\circ}\text{C}$ . However, there is no loss of weight when the temperature is above  $320\text{ }^{\circ}\text{C}$  for the purified samples. In addition, Raman spectra of blank AuSAs were also performed and no absorption peak was observed as shown in Fig. S7. These

results imply that the POEA was completely removed from the purified AuSAs.

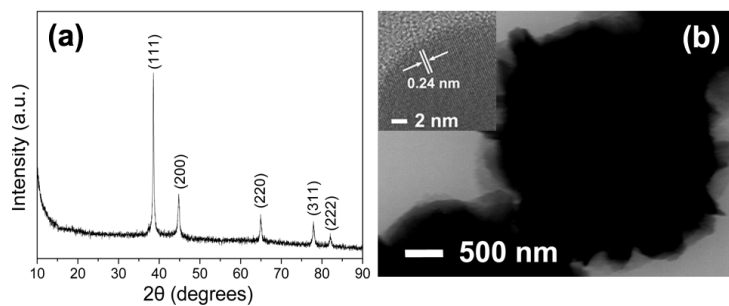


**Fig. S4** (a) XRD pattern and (b) TEM image of the purified AuSAs, the inset of (b) shows HRTEM image of the purified AuSAs.

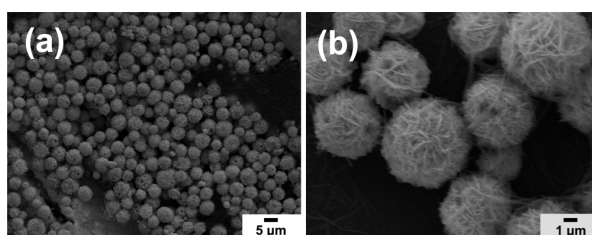


**Fig. S5** SEM images of the samples prepared at the toluene-H<sub>2</sub>O interface at shorten time of 10 min.

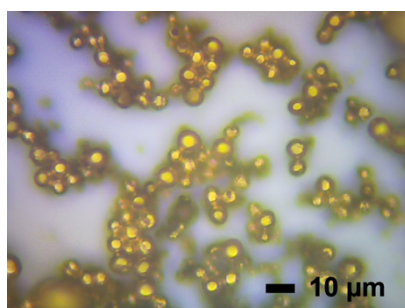


**Fig. S6** Raman image of the as-prepared AuSAs deposited on a silicon wafer substrate.

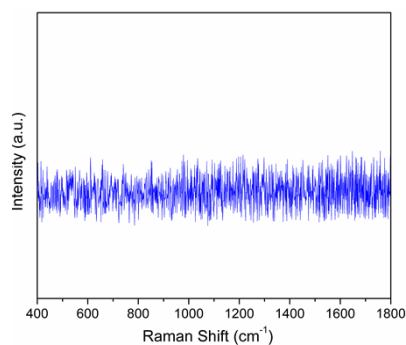


**Fig. S7** Raman spectra of the purified AuSAs.

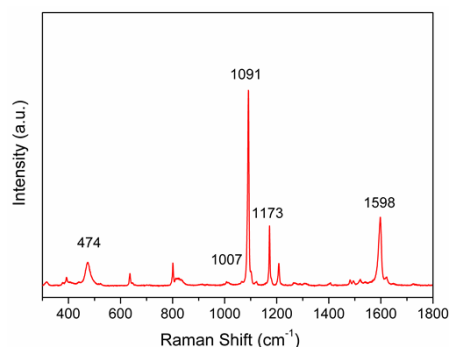


**Fig. S8** Normal Raman spectra of pure solid PAPT.

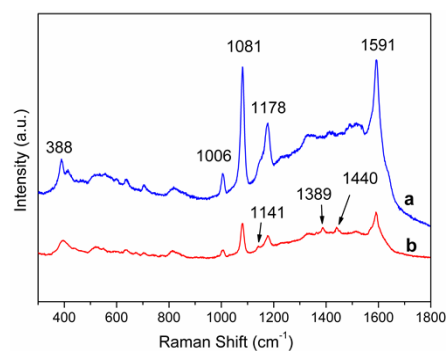


**Fig. S9** SERS spectra of PAPT adsorbed on AuSAs with different laser excitation wavelengths: (a) 785 nm, and (b) 633 nm

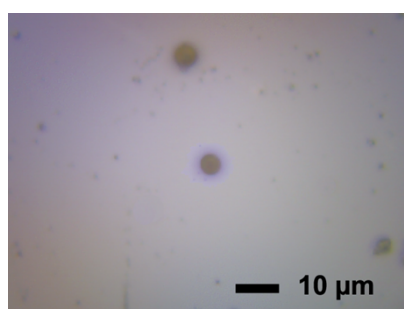


**Fig. S10** Raman image of the ultrasonic dispersed AuSAs on silicon wafer substrates.

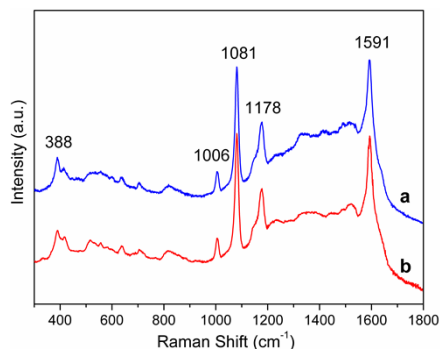


**Fig. S11** SERS spectra of PATP adsorbed on (a) directly deposited AuSAs and (b) ultrasonic dispersed AuSAs.

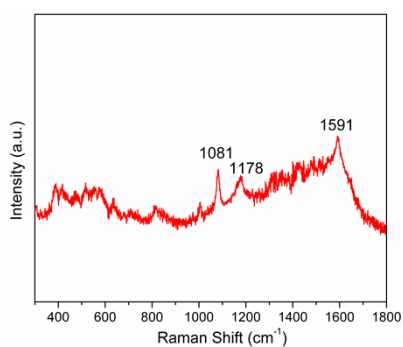


**Fig. S12** SERS spectra of PAPT adsorbed on the AuSAs at the probe molecule concentration of  $1 \times 10^{-10}$  M.

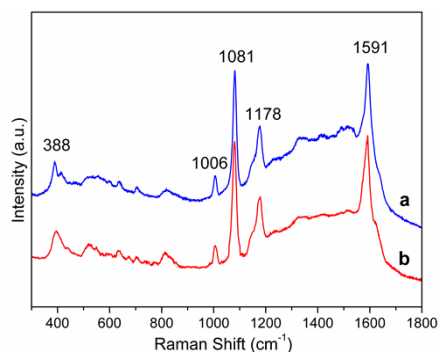


**Fig. S13** SERS spectra of PATP adsorbed on AuSAs with different storing time: (a) used directly after preparation, and (b) used after storing for six months.

**Table S1 The Main Peak Assignments, the Vibrational Bands (cm<sup>-1</sup>) of SERS and the Normal Raman Spectra of PAPT**

Assignment <sup>a, [4,5]</sup>	SERS	Normal Raman
	PAPT/AuSAs <sup>a</sup>	solid PAPT <sup>b</sup>
$\nu$ C-C, 8a (a <sub>1</sub> )	1591 (vs)	1598 (s)
$\delta$ C-H, 9a (a <sub>1</sub> )	1178 (m)	1173 (s)
$\nu$ C-S, 7a (a <sub>1</sub> )	1081 (vs)	1091 (vs)
$\gamma$ C-C + $\gamma$ C-C-C, 18a (a <sub>1</sub> )	1006 (w)	1007 (vw)
$\gamma$ C-C-C 6a (a <sub>1</sub> )		474 (s)
$\nu$ C-S	388 (s)	

<sup>a</sup> Vibrational modes:  $\nu$ , stretch;  $\delta$  and  $\gamma$ , bend.

<sup>b</sup> Relative intensity: vs, very strong; s, strong; m, moderate; w, weak; vw, very weak.

### The Calculation of SERS Enhancement factor (EF)

The detailed calculation process is shown as follows.

The EF is defined as

$$EF = (I_{surf}/N_{surf}) / (I_{bulk}/N_{bulk})$$

where  $I_{surf}$  and  $I_{bulk}$  denote the intensity of PAPT obtained with AuSAs and solid bulk PAPT, and  $N_{surf}$  and  $N_{bulk}$  are the number of PAPT molecules adsorbed on AuSAs and bulk molecules within the SERS detecting spot, respectively. For the calculation of EF values, the intensity of peaks at 1591 cm<sup>-1</sup> was used.

The spot diameter of the laser beam is about 2  $\mu$ m and its penetration depth is also about 2  $\mu$ m. Therefore,  $N_{bulk}$  can be calculated to be  $3.56 \times 10^{10}$  by using the density of the solid PAPT (1.18 g cm<sup>-3</sup>).<sup>[4,6,7]</sup> On the other hand, each PAPT molecule occupies an area of  $\sim 0.2$  nm<sup>2</sup> on full coverage of Au,<sup>[4,6,7]</sup> if we assumed a dense monolayer coverage of PAPT molecules within the laser beam,<sup>[6,7]</sup>  $N_{surf}$  can be calculated to be about  $3.9 \times 10^6$ . According to the results of the SERS measurements, the intensity ratio of  $I_{surf}$  to  $I_{bulk}$  is  $4.6 \times 10^2$ , thus the EF is calculated to be  $4.2 \times 10^6$ .

### References

- [1] A. Dawn, P. Mukherjee and A. K. Nandi, *Langmuir*, 2007, **23**, 5231.
- [2] Y. Tan, F. Bai, D. Wang, Q. Peng, X. Wang and Y. Li, *Chem. Mater.*, 2007, **19**, 5773.
- [3] M. Mazur, *J. Phys. Chem. C*, 2008, **112**, 13528.

- [4] K. Kim and J. K. Yoon, *J. Phys. Chem. B*, 2005, **109**, 20731.
- [5] X. Tang, P. Jiang, G. Ge, M. Tsuji, S. Xie and Y. Guo, *Langmuir*, 2008, **24**, 1763.
- [6] G. Lu, C. Li and G. Shi, *Chem. Mater.*, 2007, **19**, 3433.
- [7] S. Guo, L. Wang and E. Wang, *Chem. Commun.*, 2007, 3163.